

Geometrical Analysis of Crystallization of the Soft-Core Model^{*)}

Masaharu TANEMURA, Yasuaki HIWATARI,^{*,†)} Hirotugu MATSUDA,^{**}
Tohru OGAWA,^{***,†)} Naofumi OGITA^{****} and Akira UEDA^{*****}

Institute of Statistical Mathematics, Minato-ku, Tokyo 106

**Institut für Theoretische Physik, ETH, Zürich*

***Department of Biology, Faculty of Science, Kyushu University
Fukuoka 812*

****Max-Planck-Institut für Festkörperforschung, Stuttgart*

*****Institute of Physical and Chemical Research, Wako, Saitama 351*

******Department of Applied Mathematics and Physics
Faculty of Engineering, Kyoto University, Kyoto 606*

(Received February 7, 1977)

With the use of the molecular dynamics method the crystallization process from supercooled fluid states is studied for the soft-core system of the pair potential $\phi(r) = \varepsilon(\sigma/r)^{12}$, which has a simple property to characterize the relaxation towards crystalline states. The Voronoi polyhedron is introduced to examine local atomic configurations from topological point of view. Certain classes of polyhedra well characterize various phases, i.e., fluid, and bcc and fcc solids. The final relaxed state becomes a bcc crystalline state, when the system relaxes incompletely, while it becomes an fcc when the system relaxes perfectly. A unified way of defining a nucleus during the both crystallization processes is proposed. Growth of the nucleus suffers the effect of the periodic boundary condition imposed on the system.

§ 1. Introduction

According to equilibrium statistical mechanics, a solidification phenomenon is described as a first-order transition between stable fluid and solid states under constant pressure and temperature. Both phases coexist in the intermediate density region inhomogeneously. Alder and Wainwright¹⁾ first tried the molecular dynamics studies of the coexisting region of the hard-disk system. Due to the smallness of the system, however, it was difficult to estimate the equilibrium pressures of coexisting fluid and solid, respectively, with sufficient statistical accuracy. They determined the transition point by Maxwell's construction. Hoover and Ree²⁾ determined the transition point with the indirect method by introducing the single-

^{*)} The content of § 2 was reported at the International Conference on Statistical Physics held at Budapest, August 1975.

^{†)} On leave from Institute for Spectroscopic Study of Matter, Faculty of Science, Kanazawa University, Kanazawa 920.

^{††)} On leave from Department of Physics, Faculty of Science, Kyoto University, Kyoto 606.

occupancy hard-disk system and by equating the Gibbs free energies of the fluid state and of the single-occupancy system. They also applied this method to hard- and soft-sphere systems.³⁾ Since then no one seems to have successfully simulated a coexisting region of a solid-fluid transition for a three-dimensional system.

Instead, it might be possible to simulate a relaxation process towards a crystalline state from an unstable supercooled fluid state, since formation of nuclei is more abundant in a supercooled state rather than near the melting point. Actually we found that this is the case. In our previous work^{4), 5)} we studied the soft-core system with the pair potential

$$\phi(r) = \varepsilon(\sigma/r)^{12}, \quad \varepsilon > 0, \quad \sigma > 0 \quad (1.1)$$

by the molecular dynamics method.

As is well known, any reduced quantity of the system becomes a function of only a reduced density ρ^* defined by $\rho^* = \rho(\varepsilon/kT)^{1/4}$ where $\rho = N\sigma^3/V$ is the number density. Computations were made over a wide range of ρ^* . The amorphous branch of the equation of state was examined up to $\rho^* = 1.8$, with the number of atoms $N = 32$ and 108. Note that the freezing density ρ_f^* and the melting density ρ_m^* are 1.15 and 1.19, respectively.³⁾ It was found that for $N = 108$ supercooled states with $\rho^* \geq 1.3$ are unstable and compressibility factors of these states decrease with time. We also produced a motion picture showing atomic motion for one of computing runs (the run A1 in Table I) and found that the atoms eventually form a long-range order, that is, a deformed crystalline order.⁵⁾

In view of this result, we try to simulate the relaxation process from supercooled states and examine how a nucleus grows. The soft-core system with the pair potential given by Eq. (1.1) is adopted and the molecular dynamics (MD) method is applied to the system of $N = 500$ with a cubic periodic boundary. Two runs of $N = 108$ in I^{**)} (A1 and A2) are also analysed.

We introduce Voronoi polyhedra and classify the local atomic configurations from topological point of view. It is found that certain classes of polyhedra well characterize various phases, i.e., fluid, metastable fluid, and bcc and fcc solids. The final relaxed states of the system are found to be a bcc crystalline or an fcc crystalline state. The former state appears when the system relaxes incompletely, while the latter appears when it perfectly relaxes. Contrary to a macroscopic system, the simulated system itself is microscopic so that there is a problem about how to define a nucleus. Specific classes of polyhedra are found to be suitable for representation of local crystalline order and hence a way of defining a nucleus is proposed. Particularly, when the system relaxes towards a bcc crystalline state, a nucleus is most uniquely defined. In this case, the time variation of a nuclear size is well correlated with that of the instantaneous compressibility factor. For

^{*)} Hereafter referred to as I.

^{**)} In Tables I and II of I, the averaged values for unstable states are given incorrectly without consideration of their relaxation towards crystalline states.

the relaxation to an fcc crystalline state, a nucleus is similarly defined with some manipulation. We also examined the structure of nuclei with *XY*-plotter output and found that the nucleation proceeds even one-dimensionally when they grow rather abruptly. This indicates that the periodic boundary condition affects the crystallization process for such a small system.

In the next section we first remark a certain property of the soft-core system which characterizes the relaxation and then give the method and the result of our computation on the crystallization processes. In §3 we introduce Voronoi polyhedra to represent local atomic configurations in various phases. In §4 we propose a way of defining a nucleus and present the time evolution of nuclei. Finally we discuss our results in §5.

§ 2. Relaxation of the soft-core system towards crystalline state

We simulate the crystallization process as a relaxation process toward a crystalline state from an unstable supercooled fluid state. In connection with this process, the soft-core system has some interesting characteristics when combined with the MD method. First, as stated in §1, any reduced thermodynamical quantity becomes a function of only ρ^* . Secondly, the instantaneous compressibility factor $(PV/NkT)_t$, where the subscript t hereafter denotes the value of the quantity at time t , which is defined by the same relationship (see Eq. (4.1) in I) as that derived from the virial theorem, has a simple form:

$$\left(\frac{PV}{NkT}\right)_t = 1 + \frac{12\varepsilon}{3NkT_t} \left[\sum_{i < j} (\sigma/r_{ij})^{12}\right]_t = 1 + 6\frac{U_t}{K_t}, \quad (2.1)$$

where K_t and U_t are the kinetic and the potential energies, respectively, and $U_t = \varepsilon[\sum_i \sum_{i < j} (\sigma/r_{ij})^{12}]_t$. The instantaneous temperature T_t is defined by $kT_t = 2K_t/3N$. Since in the MD method the equations of motion are integrated without use of any manipulation, the total energy $E = K_t + U_t$ is conserved in the course of a computation. Since also the density ρ is kept constant, Eq. (2.1) can be rewritten as

$$\left(\frac{PV}{NkT}\right)_t = 6\frac{E}{K_t} - 5 = 4\frac{E}{N} \left(\frac{\rho_t^*}{\rho}\right)^4 - 5 \equiv g(\rho_t^*), \quad (2.2)$$

where $\rho_t^* = \rho(\varepsilon/kT_t)^{1/4}$. Therefore, $(PV/NkT)_t$ becomes a function of only K_t or ρ_t^* , which we denote by $g(\rho_t^*)$ for simplicity.

It should be noted that from the above discussion a simulating state moves always along a unique path in the $g(\rho_t^*)$ - ρ_t^* plane. The path which passes a state of point $(\rho_0^*, g(\rho_0^*))$ in the plane at an initial time $t=0$ is given, from Eq. (2.2), by

$$g(\rho_t^*) = [g(\rho_0^*) + 5] \left(\frac{\rho_t^*}{\rho_0^*}\right)^4 - 5. \quad (2.3)$$

If an initial state $(\rho_0^*, g(\rho_0^*))$ is unstable, the state relaxes towards its equilibrium

state along the path given by Eq. (2.3). Actually, this fact was confirmed in our simulation.

In order to prepare the initial amorphous fluid states, one of phases of an equilibrium fluid state at high density is first picked up and the rapid cooling and/or compression methods are applied, of which details are given in I. For $N=108$, initial phases used for the runs *A1* and *A2* were stable fluids of densities $\rho=0.9$ and $\rho=0.85$, respectively. To the run *A1* a compression method was applied, whereas a cooling method was applied to the run *A2*. For $N=500$, the initial phases used for preparation of the initial states are two equilibrium fluid states whose densities are $\rho=0.9$ and whose temperatures are $kT/\varepsilon=0.494$ and 0.434 . The compression and cooling methods are applied. The initial states, just after cooling and/or compression, for computation are summarized in Table I where the run of a metastable state (*B0*) is also given.

Table I. Summary of data of initial states used in the computations for $N=108$ and 500 . Suffix \circ represents the initial values. For the definition of time step, see I. In the Table, the corresponding eventual states due to Eq. (2.3) are also given for respective runs through the suffix ∞ .

N	ρ	time steps	ρ_0^*	$(PV/NkT)_0$	kT_0/ε	ρ_{∞}^*	$(PV/NkT)_{\infty}$	state	reference
108	1.87	1300	1.64 ₆	58.55	1.662	1.45	33.80	unstable	<i>A1</i>
108	0.85	2000	1.49 ₆	44.16	0.104	1.32	25.03	unstable	<i>A2</i>
500	1.10	10000	1.34 ₆	30.69	0.442	1.25	21.48	metastable	<i>B0</i>
500	1.11	5000	1.36 ₂	31.32	0.441	1.27	22.40	unstable	<i>B1</i>
500	1.12	5000	1.37 ₇	32.57	0.438	1.28	22.70	unstable	<i>B2</i>
500	1.13	5000	1.33 ₆	29.56	0.512	1.25	21.45	unstable	<i>B3</i>

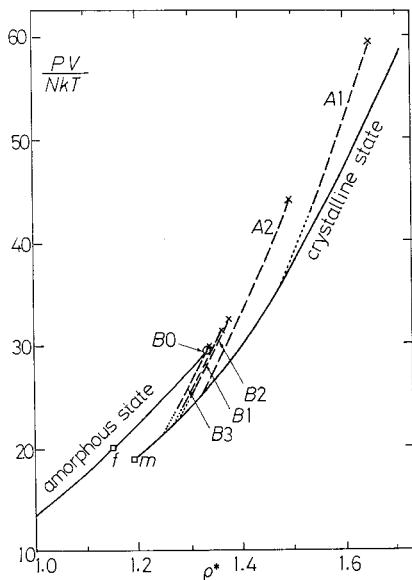


Fig. 1. Equation of state of soft-core system at high densities. Solid curves are amorphous and fcc crystalline states, respectively. Reference marks are accompanied for the runs in the present work. \square : freezing and melting points, \times : initial phase for an unstable state, \circ : metastable state (run *B0*). ----: relaxation path given by Eq. (2.3) along which an unstable state moved,: relaxation path where an unstable state will pass if the state relaxes completely.

Figure 1 shows the equation of state at high densities. The amorphous and fcc crystalline states are represented by the solid curves, respectively, by joining the points obtained by Hoover et al.³⁾ and by Ogura et al.⁶⁾ both with the Monte Carlo method, and those of I. In the Figure, the freezing and melting points are designated by open squares. The open circle represents the metastable state (*B0*). The initial phases (indicated by crosses) of unstable states lie almost on a single curve extrapolated smoothly from the amorphous branch. The path of Eq. (2.3) which crosses the crystalline branch at melting point ρ_m^* intersects with the branch of metastable fluid phase at $\rho^* \simeq 1.28$.

Relaxation towards stable states depends much on the initial unstable states. In Fig. 1, the relaxation paths given by Eq. (2.3) are illustrated for respective runs. In order to examine the relaxation, we conventionally introduce a relaxation function $\Phi(t)$,⁷⁾ i.e.,

$$\Phi(t) = \frac{g(\rho_i^*) - g(\rho_\infty^*)}{g(\rho_0^*) - g(\rho_\infty^*)} \quad (2.4)$$

for a single computing run. The value of $g(\rho_\infty^*)$, the compressibility factor of an eventual ($t \rightarrow \infty$) crystalline state, can be determined as an intersection between the curve of $g(\rho_i^*)$ and of the equation of stable crystalline states by virtue of Eq. (2.3) without knowledge of time dependence of $g(\rho_i^*)$.

Figure 2 represents the relaxation function $\Phi(t)$ for each run, where dots show the values averaged over 50 time steps for $N=108$ and over 100 time steps for $N=500$. Note that one time step is equal to 10^{-14} sec, if one uses data of Ar for ε , σ and the atomic mass. The $\Phi(t)$'s for the runs *A1* and *A2* show initially a rather rapid decrease towards more stable states. The run *A2* shown in Fig. 2(b) is a typical example of complete relaxation to a crystalline state and its $\Phi(t)$ relaxes to zero completely. On the other hand, the $\Phi(t)$ in Fig. 2(a) (the run *A1*) stays in an incompletely relaxed state for a long period. In the former case the analysis of the spatial atomic configuration of its final stable state reveals that the state is a complete fcc crystalline.

For the run *B0* the $\Phi(t)$ fluctuates, but does not show any tendency of decrease up to 10000 time steps and hence the state simulated can be regarded as metastable. On the other hand, the $\Phi(t)$ for the runs *B1*, *B2* and *B3* maintain values slightly lower than those of initial states for a while and then begin to decrease to more stable states. For the run *B2* the decrease to a more stable state is not yet accomplished within a computing time. These tendencies indicate the fact the relaxation has initiated from the unstable state towards the more stable state.

For the 500-atom system we have not yet obtained a run which relaxes to an fcc state (see Figs. 2(d), (e) and (f)). The final states of *B1* and *B3* are shown to be incomplete bcc crystalline states as will be seen later.

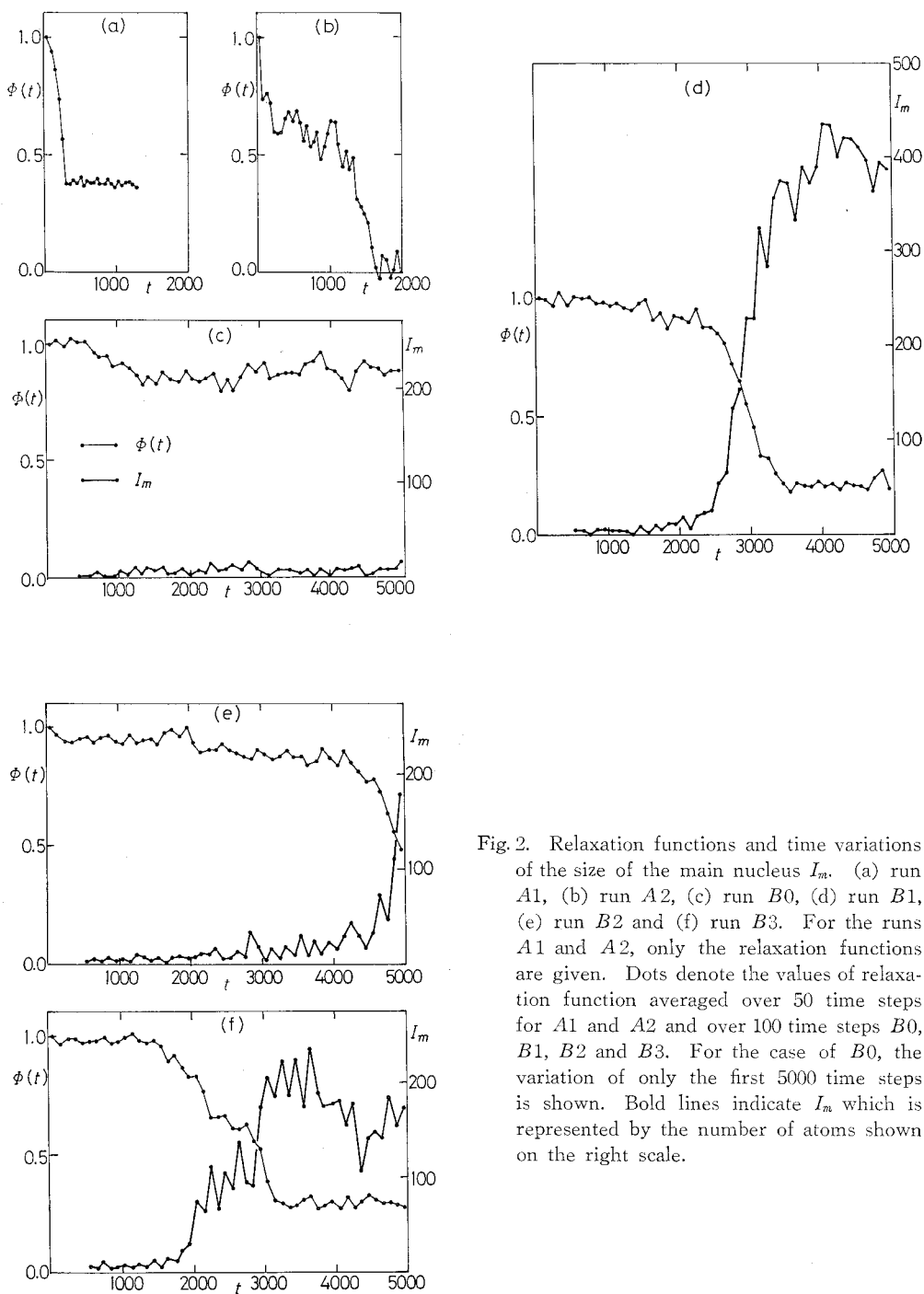


Fig. 2. Relaxation functions and time variations of the size of the main nucleus I_m . (a) run A1, (b) run A2, (c) run B0, (d) run B1, (e) run B2 and (f) run B3. For the runs A1 and A2, only the relaxation functions are given. Dots denote the values of relaxation function averaged over 50 time steps for A1 and A2 and over 100 time steps B0, B1, B2 and B3. For the case of B0, the variation of only the first 5000 time steps is shown. Bold lines indicate I_m which is represented by the number of atoms shown on the right scale.

§ 3. Geometrical classification of local atomic configurations

To examine how the crystallization process develops in the computer simulation, we have to define a crystalline nucleus in the system. There might exist differences in local order and in local density between the nuclei and the remained parts. However the difference in local density may be small (see § 5), contrary to a rather large difference in density between gas and liquid in case of condensation. We find it convenient to employ the "Voronoi polyhedra".⁹⁾ They have been frequently used in various fields. Particularly, Bernal,⁹⁾ Rahman¹⁰⁾ and Finney¹¹⁾ used them to represent liquid structures. Two of us also used its dual concept of them (Delaunay figures) for representation of a hard-core system.¹²⁾ For a given configuration $\{\mathbf{r}_i, i=1, 2, \dots, N\}$ of N atoms, there corresponds one Voronoi polyhedron Π_i to each atom i . The Π_i of atom i is defined as a set of all points of space which are closer to the position \mathbf{r}_i than to any $\mathbf{r}_j (j \neq i)$. The boundaries of the polyhedron are evidently consisting of faces which are some of the $N-1$ perpendicular bisectors of the line segments $\mathbf{r}_{ij} (= \mathbf{r}_j - \mathbf{r}_i), j=1, \dots, N (\neq i)$. It is easily seen that all polyhedra are convex. The set of all the polyhedra fill the space uniquely. This is a generalized version of Wigner-Seitz cell.

The volume of a polyhedron Π_i would be a good measure for the local atomic volume, i.e., local atomic density. The geometrical structure of Π_i represents the local atomic configuration around the atom i , which is our main concern.

We define the atom, say j , is contiguous to the atom i , if the perpendicular bisector of the line segment \mathbf{r}_{ij} constitutes a face of Π_i . The pair of atoms i and j which are contiguous to each other, are said to be a contiguous pair. Now, let us denote the total number of faces of a polyhedron for an atom by f . It is equal to the number of atoms contiguous to the atom. Then, f represents a local coordination number.¹³⁾ To represent local configurations, we need further informations about the arrangement of atoms around the atom. We note that for a given Π_i the number of edges of a face, through which an atom j confronts to the atom i , indicates the number of circumferential atoms which are contiguous

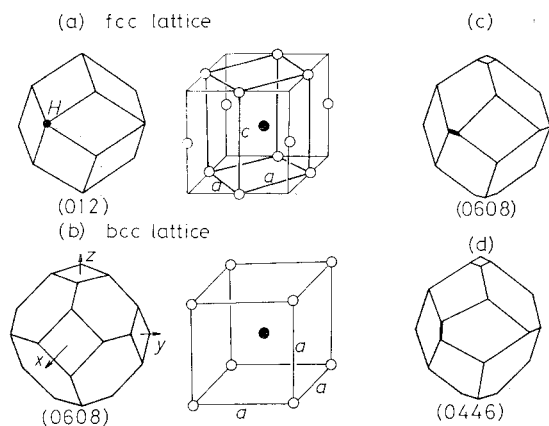


Fig. 3. Topological relations between fcc and bcc lattices and between (0608)- and (0446)-polyhedra. (a) fcc lattice, (b) bcc lattice. Black circles are the centered atoms of respective Voronoi polyhedra. If the parallelepiped indicated by bold lines in (a) is compressed from top and bottom, it turns out to the unit cell of (b). (c) (0608)-polyhedron, (d) (0446)-polyhedron. If the horizontal bold line is replaced by the vertical, the (0608)-polyhedron changes to the (0446)-polyhedron and vice versa.

to both i and j . A set of these numbers of II_i represents more detailed local atomic arrangements around the atom i . We, therefore, introduce an index defined by a set of integers $(n_3 n_4 n_5 \dots)$ for an f -faced polyhedron in accord with Finney,¹¹ where $n_\alpha (\alpha \geq 3)$ is the number of α -sided faces (that is, faces whose number of edges is equal to α) and $f = \sum_\alpha n_\alpha$. For example, as shown in Figs. 3(a) and (b), the Voronoi polyhedron of an fcc crystal lattice is a rhombic dodecahedron of which index is given by $(0\ 12\ 0\ 0\ 0\ \dots)$, while that of bcc lattice is a truncated octahe-

Table II(a). Axes of crystalline nuclei (main clusters) in cases of $B1$ and $B3$. Direction cosines and lattice constants are derived with the use of coordinates of atoms averaged over 50 time intervals from the specified time steps. Lattice constants are measured in unit of σ . The numbers of (0608)-atoms represent those in the averaged atomic configurations.

ρ	time step	direction cosine			lattice constant	No. of (0608)-atoms
1.11	1800	(0.692	0.685	-0.214)	1.179	4
		(0.405	-0.074	0.902)	1.273	
		(-0.625	0.694	0.343)	1.330	
	2200	(0.720	0.645	-0.220)	1.209	9
		(0.416	-0.163	0.889)	1.258	
		(-0.555	0.739	0.362)	1.222	
	2500	(0.702	0.659	-0.240)	1.272	20
		(0.436	-0.140	0.879)	1.231	
		(-0.552	0.726	0.389)	1.187	
	3100	(0.736	0.623	-0.230)	1.244	239
		(0.409	-0.163	0.888)	1.241	
		(-0.528	0.749	0.384)	1.182	
3900	(0.728	0.631	-0.227)	1.246	321	
	(0.418	-0.149	0.886)	1.255		
	(-0.534	0.746	0.376)	1.170		
1.13	1900	(0.470	0.786	0.389)	1.220	9
		(0.586	-0.603	0.521)	1.187	
		(-0.653	0.038	0.750)	1.285	
	2000	(0.495	-0.758	-0.392)	1.176	19
		(0.510	0.631	-0.571)	1.168	
		(-0.689	-0.105	-0.636)	1.314	
	2100	(0.465	-0.767	-0.421)	1.183	26
		(0.518	0.626	-0.567)	1.185	
		(-0.707	-0.074	-0.691)	1.279	
	3900	(0.514	-0.757	-0.373)	1.141	66
		(0.395	0.585	-0.691)	1.197	
		(-0.754	-0.206	-0.616)	1.330	

dron with index (060800...). If 0's continue infinitely, we omit these for simplicity and denote (060800...), for instance, by (0608). The atom whose polyhedron has an index $(n_3 n_4 n_5 \dots)$ will be said as $(n_3 n_4 n_5 \dots)$ -atom. It will be shown that these indices play an important role for our purposes.

In order to characterize atomic configurations we eliminate the effect of thermal oscillations by averaging atomic positions over 50 time steps (see Table II(a)). In all cases the configuration thus obtained is used for the analysis. Note that a period of Einstein oscillation corresponds to a few ten time steps at densities we are concerned.

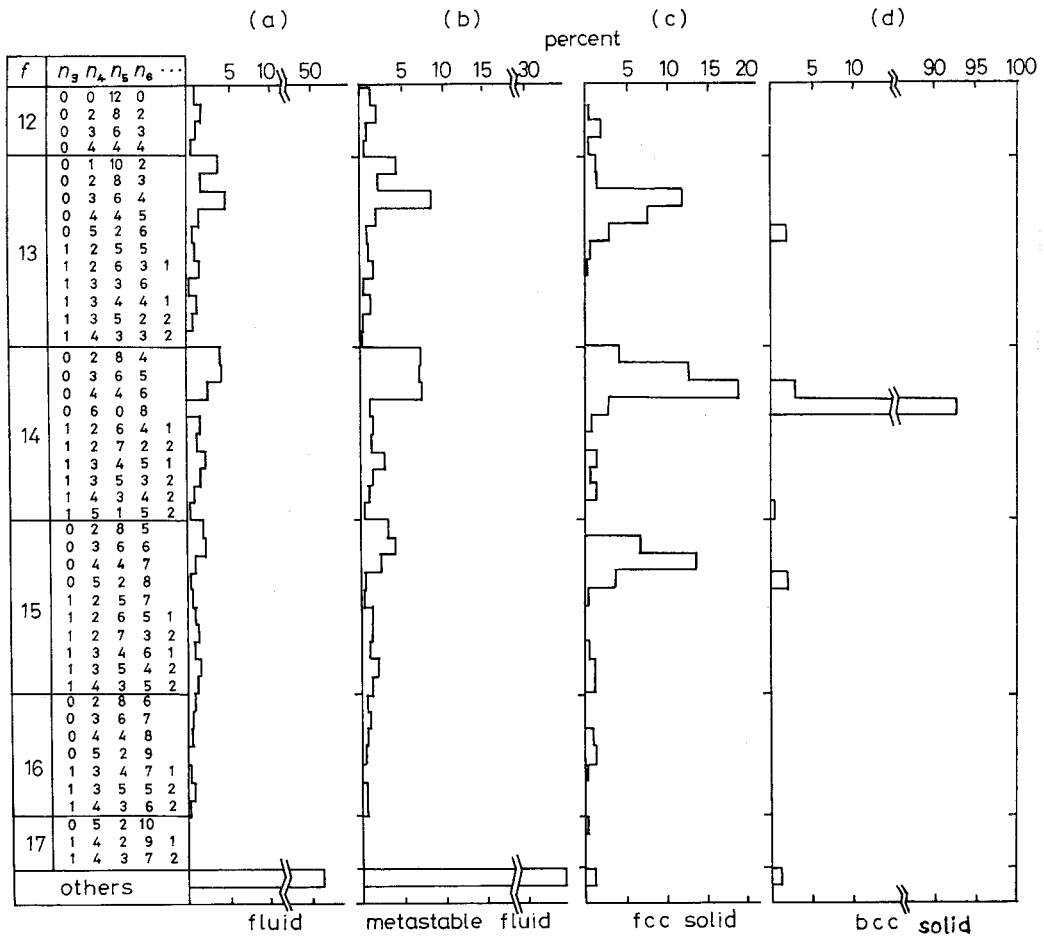


Fig. 4. Histograms showing the fractions of Voronoi polyhedra classified according to the sets of integers $(n_3 n_4 n_5 \dots)$ for various phases. (a) fluid, $\rho=0.90$, $N=500$ ($\rho^*=1.12$).¹⁴⁾ (b) metastable fluid (run B0). (c) fcc solid, $\rho=1.25$, $N=256$ ($\rho^*=1.50$). (d) bcc solid, $\rho=1.25$, $N=250$ ($\rho^*=1.51$). The numbers of polyhedra used for statistics are 6500 for case (a), 5000 for case (b), 512 for case (c) and 1500 for case (d). The cases (c) and (d) were simulated separately from the runs in the text. Polyhedra which are of minor abundance and hence not listed are gathered in the item "others".

We first show the result about fluid and solid states. Figure 4 gives typical histograms of polyhedra classified according to the above-mentioned indices for fluid ($\rho=0.9$), metastable fluid ($\rho=1.10$, the run *B0*), fcc solid ($\rho=1.25$) and bcc solid ($\rho=1.25$). The first column gives the number of faces of polyhedra and the second shows the indices at given number of faces. The fluid phase and metastable fluid phase exhibit similar histograms, where many classes of polyhedra appear but the abundance of polyhedra of each index is small; the most abundant one is at most 10%, though it depends on the density ρ . Solid phases, as compared with fluid phases, show different histograms depending on the type of a crystalline lattice. Figure 4(c) shows that an fcc solid has various classes of polyhedra such as (0 3 6 4), (0 3 6 5), (0 4 4 6) and (0 4 4 7), whose abundances exceed 10%, while Fig. 4(d) (bcc solid) shows that about 90% of polyhedra are of class (0 6 0 8). The difference between fcc and bcc solids appears from the fact that

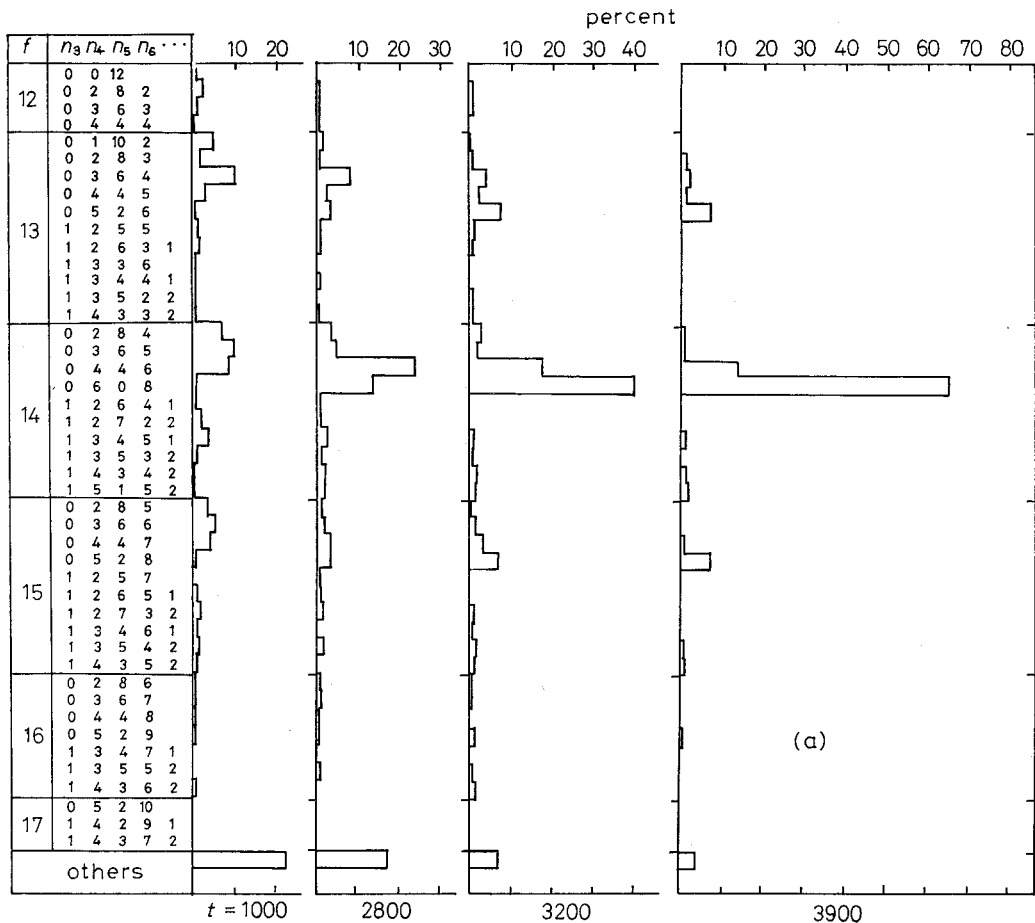


Fig. 5. (Figure captions are printed on the next page.)

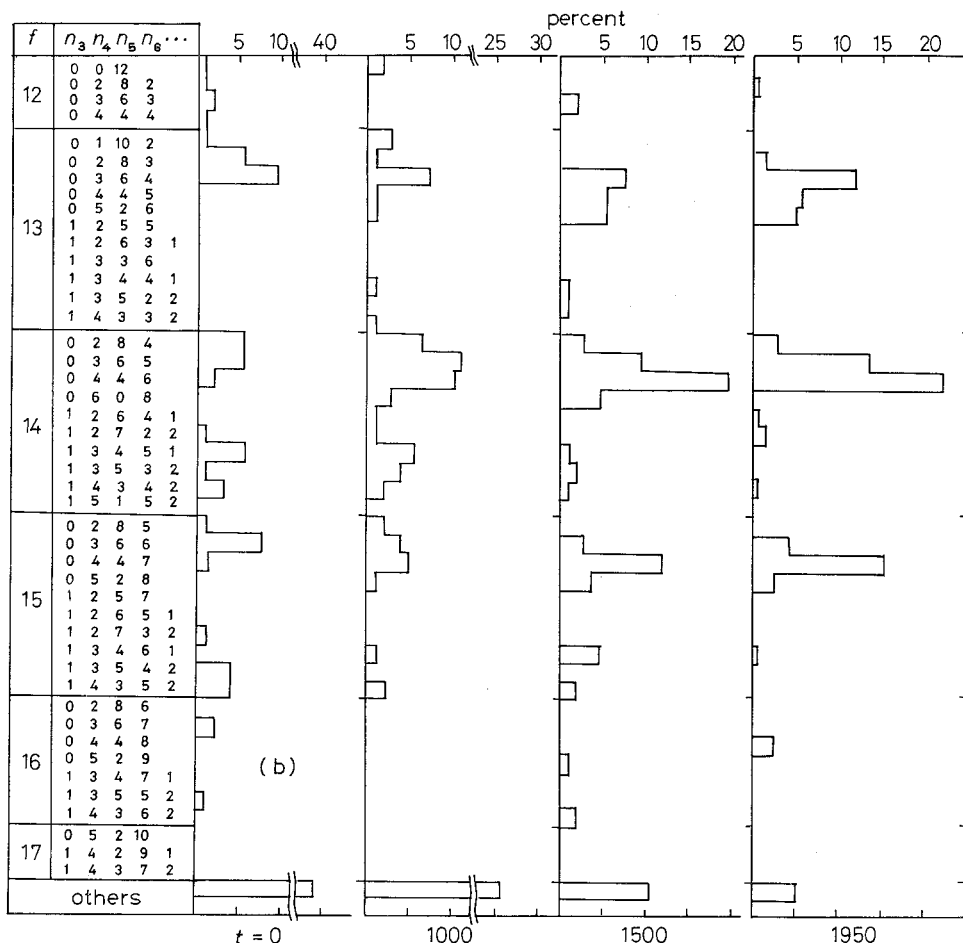


Fig. 5. Time variations of the fractions of Voronoi polyhedra. (a) run B1, (b) run A2.

truncated octahedra in the bcc lattice, i.e., (0608)-atoms are stable^{*)} with respect to random displacements of the atoms due to thermal oscillations, whereas rhombic dodecahedra in the fcc lattice, i.e., (012)-atoms are quite unstable^{*)} with respect to those displacements and transform to various abundant classes of polyhedra observed in the fcc solid (see also Appendix I).

Next we apply the same analysis to the crystallization processes. Figure 5(a) shows the time variation of the histograms of polyhedra for the run B1. As time goes on, the number of (0446)-atoms first increases, then subsequently the number of (0608)-atoms tends to increase and soon exceeds that of (0446)-atoms. Finally (0608)-atoms overwhelm the atoms of other classes. It is clearly seen

^{*)} A polyhedron is called stable, if a slight movement of neighbouring atoms does not change the topology of the polyhedron, and is called unstable if it does.

Table II(b). Lattice constants of perfect fcc and bcc crystals at the same densities as those of *B1* and *B3*, respectively. The lattice constants of fcc lattice are given by the lengths of the two sides (indicated by *a* and *c*) of the rectangular parallelepiped and those of bcc lattice by the length of the side (indicated by *a*) of the unit cell shown in Fig. 3, respectively.

ρ	lattice constant	
	fcc	bcc
1.11	1.084	1.217
	1.084	1.217
	1.533	1.217
1.13	1.078	1.210
	1.078	1.210
	1.524	1.210

that the last histogram resembles closely to that of a bcc solid. From the values of lattice constants given in Tables II(a) and (b) (see also later arguments), it is concluded that the crystalline structure of the relaxed state is bcc with an anisotropic deformation. Figure 5(b) represents the time variation of the histogram for the run *A2* which relaxes completely. The general feature of the histogram is quite different from that of *B1*. As the relaxation proceeds, the number of (0 4 4 6)-atoms and of some other classes of atoms increase and the histogram eventually becomes similar to that of an fcc solid (its similarity is confirmed by the chi-square test). Therefore, the completely relaxed state can be regarded as an isotropic fcc solid. The reason why the final relaxed state is bcc if the system relaxes incompletely is explained in Appendix II. The results so far obtained show that the use of Voronoi polyhedra well characterize the various phases, particularly crystalline states.

§ 4. Crystalline nucleus and crystallization process

Let us first consider how to define a nucleus in a system which relaxes towards a bcc solid. As shown in case *B1*, if a relaxed state is bcc, (0 6 0 8)- and (0 4 4 6)-polyhedra are expected to play an important role for nuclear growth. The topological relation between these polyhedra is illustrated in Fig. 3. If the bold vertical edge of the (0 4 4 6)-polyhedron changes to a bold horizontal edge, a (0 4 4 6)-atom turns out to a (0 6 0 8)-atom and vice versa. This change is caused by a slight movement, that is, a thermal oscillation of contiguous atoms. In this sense, a (0 4 4 6)-atom is akin to a (0 6 0 8)-atom. When the system relaxes towards an isotropic fcc state, however, these atoms have no longer a relation to nuclear growth as shown in case *A2*. However, in this case, we can also realize the same situation as in the case of a bcc solid by compressing the system slightly parallel to one of the axes of fcc crystalline lattice of the system so that it relaxes to a bcc solid with anisotropic distortion (see Appendix II). Since an fcc

solid has a topologically intimate relation to a bcc solid, applying the deformation to the system at any instant during relaxation may change nuclei to those which consist of polyhedra of the same classes as in case of a bcc solid. Therefore, to both types of relaxation towards a bcc solid and a fcc solid, we may apply the same definition of a nucleus which is described as follows:

Definition of crystalline nucleus

1. A nucleus contains at least one (0608)-atom.
2. If (0608)-atoms and/or (0446)-atoms are contiguous to a (0608)-atom, they are included to the nucleus of the latter.
3. The number of the both kinds of atoms in a nucleus represents the nuclear size.

On the basis of this definition, we investigate the time variation of the size of nuclei for the runs *B1*, *B2* and *B3*. In Figs. 2(d), (e) and (f), the time evolutions of the largest nucleus*¹ (main cluster), I_m , are presented. Bold lines represent the time dependences of I_m . The nucleus begins to grow gradually until it becomes a few tens and then grows rapidly. The time dependence of $\Phi(t)$ is well correlated with this feature. At the early stages of crystallization, there exist several nuclei whose sizes are small and comparable to each other. Later on one of them grows up as a main nucleus and the other nuclei are unified to the main. Figures 6(a), (b) and (c) show the spatial distributions of nuclei at early stages of crystallization for the run *B1*. Solid circles represent (0608)-atoms, while dotted circles represent (0446)-atoms. The position of atoms in the direction perpendicular to the figure is represented by the size of a circle. Solid segments connect the contiguous pairs of both (0608)-atoms, while broken segments connect between (0608)-atoms and their contiguous (0446)-atoms. In this way a set of atoms which are connected with each other forms a nucleus as defined above.

Direction cosines of axes and lattice constants of nuclei can be determined as follows: As is shown in Fig. 3(b), each of the four-sided faces of the (0608)-polyhedron has respective axis as a normal. Finding the normals of six four-sided faces of each (0608)-polyhedron in a nucleus, we calculate the direction cosines of the three axes and lattice constants. Table II(a) gives the averages of these values for the runs *B1* and *B3*. At early stages of crystallization, there already appears a gross feature similar to that of the main nucleus of later stages. The lattice constants are different in the three directions, but the orthogonality of the three axes is well realized. They should be compared with those of the perfect fcc and bcc lattices. The lattice constants at the same densities are given in Table II(b). Comparison shows that a crystalline part(nucleus) seems to be too distorted to identify it as an fcc structure. It has a structure close to a bcc structure with

*¹ Due to the smallness of the system size, it is found that nuclei other than the largest one are too small to be called nuclei except the early stage of the crystallization process.

anisotropy.

An analysis of nuclear growth when a system relaxes to an fcc solid, with the use of the definition, will be treated separately.

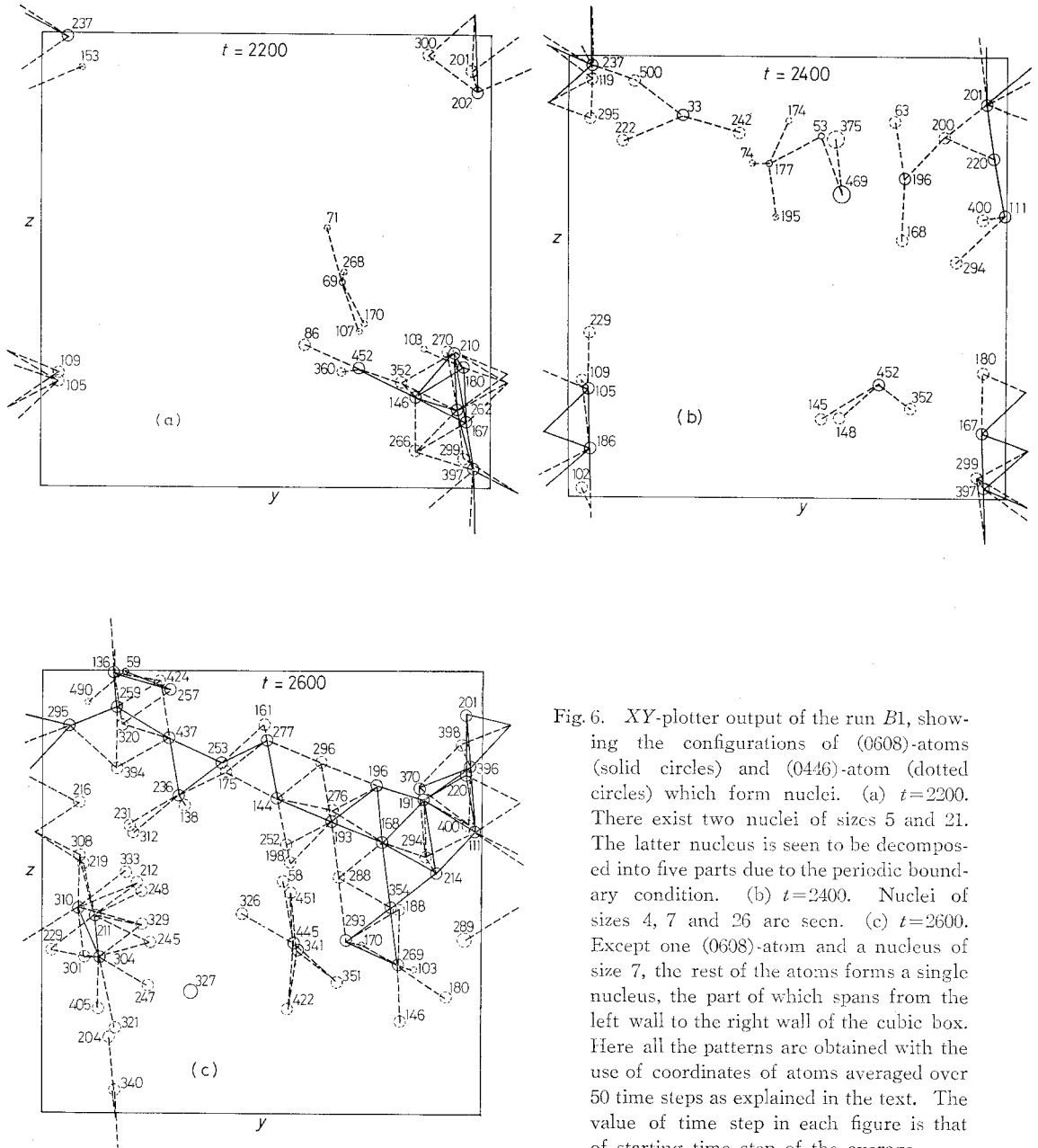


Fig. 6. XY-plotter output of the run B1, showing the configurations of (0608)-atoms (solid circles) and (0446)-atom (dotted circles) which form nuclei. (a) $t=2200$. There exist two nuclei of sizes 5 and 21. The latter nucleus is seen to be decomposed into five parts due to the periodic boundary condition. (b) $t=2400$. Nuclei of sizes 4, 7 and 26 are seen. (c) $t=2600$. Except one (0608)-atom and a nucleus of size 7, the rest of the atoms forms a single nucleus, the part of which spans from the left wall to the right wall of the cubic box. Here all the patterns are obtained with the use of coordinates of atoms averaged over 50 time steps as explained in the text. The value of time step in each figure is that of starting time step of the average.

§ 5. Discussion

As shown in the previous sections, the description by Voronoi polyhedra demonstrates its ability for analyses of crystallization process which proceeds inhomogeneously in space. The analyses were made from a topological point of view. We also investigated the volume distribution of polyhedra in order to examine whether nuclei and other portions can be distinguished in terms of their volume difference. However the answer was negative, since the average volume difference was found only about one percent, partly because the density of the system we are concerned is already high and partly because the density change at the fluid-solid transition is small.

Recently, crystal nucleation in a Lennard-Jones system has been reported by Mandell et al.¹⁶⁾ for $N=108$. Computations were performed by an MD method and a cooling method was applied to prepare supercooled fluids. They observed the time variation of instantaneous structure factor $S(\mathbf{k})$ for a specified wave vector \mathbf{k} and concluded a state to be crystalline when $S(\mathbf{k})$ reaches a value of order N^2 for a special reciprocal lattice vector. Though $S(\mathbf{k})$ may be conveniently used for theoretical approach to crystallization, in order to examine how a nucleus grows, the use of Voronoi polyhedra seems to provide a more direct information than $S(\mathbf{k})$ does. The system size, $N=108$ in their case, or even 500 in our case, appears too small as will be discussed later.

Here we remark two facts about our results. First, since the system is simulated with the use of the MD method with constant total energy and density, crystallization does not proceed at constant pressure, but accompanies with a temperature rise. This might affect to suppress the production rate of nuclei. Secondly, due to the periodic boundary condition employed, crystallization proceeds in a sort of external periodic potential field. This artificial field might affect to increase the growth rate of a nucleus. There is an evidence, as Fig. 6 shows, that a nucleation proceeds anisotropically. Though the size of a nucleus is small, the nucleus extends one-dimensionally from one side to the other of the cubic box in which the system is confined. In case of a 500-atom system, about eight atoms are arranged along a side of the box. Therefore, the crystallization process suffers the effect of the periodic boundary condition. As far as the initial stages of nucleation is concerned, at which the size of the main nucleus is much smaller than the system size, the effect may be small. However the effect is crucial for the further growth of the nucleus.

As shown in Fig. 2, the main cluster size I_m first increases gradually until it becomes a few tens and then grows rapidly. If the system would be large enough, that size could be identified as a critical size. Due to the smallness of the system size, however, it is difficult to ascertain a true critical size. In order to examine the effect, computation for a larger system is required.

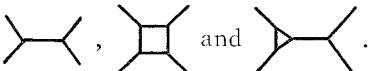
Acknowledgements

The authors express their hearty thanks to Mr. M. Noguchi for his assistance in computations. One of the authors (M. T.) thanks to Professor T. Matsubara, Kyoto University, for critical reading and also to Professor I. Higuti, Institute of Statistical Mathematics (ISM), for his continuing encouragements. Numerical computations were carried out on the computers of the Institute of Physical and Chemical Research as well as that of ISM. This work was partially financed by the Scientific Research Fund of the Ministry of Education and by the Research Institute for Fundamental Physics, Kyoto University, as a research project.

Appendix I

—Instability of a (0 12)-Polyhedron—

From the definition of H_i given in § 3, a vertex of H_i is determined as an intersecting point of faces. In most cases the number of the faces meeting at a vertex is three, but, as shown in Fig. 3(a), at a vertex H of (0 12)-polyhedron four faces meet. Therefore, when the atoms are displaced from respective lattice points due to thermal oscillation, the vertex H is immediately decomposed into several vertices. If the displacement is sufficiently small compared with the lattice constants, the vertex

H is decomposed into two or four vertices such as 

Since there are six vertices of H type, decomposition of these vertices produces various types of polyhedra of which number of faces ranges from $f=12$ to 18.¹⁶⁾

Appendix II

—Topological Relation of Voronoi Polyhedra between fcc and bcc Solids—

In the appearance of histograms showing various classes of polyhedra, fcc and bcc solids are clearly distinguishable from each other. However there is a continuous way to connect between them topologically. In Fig. 3 unit cells of fcc and bcc lattices are presented. The Voronoi polyhedra of centered atoms (black circles) are shown, respectively, on the left side. If the fcc lattice is compressed from top and bottom along the (001)-axis, i.e., the c -axes indicated by bold lines, the (0 12)-polyhedron is transformed to a polyhedron such as (0 6 0 8) (compare with Figs. 3(a) and 3(b)). When the compression is continued until a length along the c -axes becomes $1/\sqrt{2}$ of the original one, the rectangular parallelepiped shown by bold lines changes to the unit cell of a bcc lattice, that is, the fcc lattice is completely transformed to a bcc lattice.^{*)} However, the trans-

*) This deformation is called Bain's deformation.^{17), 18)}

formed (0608)-polyhedron is no more transformed to any other by the compression. Therefore, if an fcc solid is compressed along the (001)-axis by more than amplitudes of thermal oscillation, its histogram of polyhedra must resemble to that of a bcc solid.

When the system relaxes completely to an fcc solid, there are certain directions of the fcc crystalline axis which are compatible with the periodic boundary condition. Among such axes, we find one of the (001)-axes and then apply the above-mentioned compression along the axis to the system. In this way, we can examine nuclei in the system by observing those in the deformed system with the use of (0608)- and (0446)-polyhedra.

When a nucleus is growing, if its crystalline axes are not compatible with the periodic boundary condition, the system is affected to compress along one of the axes by the condition, and hence the system cannot relax completely. The final relaxed state, therefore, becomes bcc crystalline with anisotropy.

References

- 1) B. J. Alder and T. E. Wainwright, *Phys. Rev.* **127** (1962), 359.
- 2) W. G. Hoover and F. H. Ree, *J. Chem. Phys.* **47** (1967), 4873.
- 3) W. G. Hoover and F. H. Ree, *J. Chem. Phys.* **49** (1968), 3609.
W. G. Hoover, M. Ross, K. W. Johnson, D. Henderson, J. A. Barker and B. C. Brown, *J. Chem. Phys.* **52** (1970), 4931.
W. G. Hoover, S. G. Gray and K. W. Johnson, *J. Chem. Phys.* **55** (1971), 1128.
- 4) Y. Hiwatari, H. Matsuda, T. Ogawa, N. Ogita and A. Ueda, *Prog. Theor. Phys.* **52** (1974), 1104. (This is referred to as I.)
- 5) T. Ichimura, A. Ueda, T. Ogawa, N. Ogita, H. Ogura, M. Tanemura, Y. Nakagawa, Y. Hiwatari and H. Matsuda, reported at the 28th annual meeting of Phys. Soc. Japan, April 1973.
- 6) H. Ogura, T. Ogawa, N. Ogita, H. Matsuda and A. Ueda, *Prog. Theor. Phys.* **58** (1977), 419.
- 7) K. Binder, *Phys. Rev.* **B8** (1973), 3423.
- 8) C. A. Rogers, *Packing and Covering*, (Cambridge Univ. Press, Cambridge, 1964), Chap. 7.
- 9) J. D. Bernal, *Nature* **183** (1959), 141.
J. D. Bernal and J. L. Finney, *Disc. Farad. Soc.* **43** (1967), 60.
- 10) A. Rahman, *J. Chem. Phys.* **45** (1966), 2585.
- 11) J. L. Finney, *Proc. Roy. Soc.* **A319** (1970), 479, 495.
- 12) T. Ogawa and M. Tanemura, *Prog. Theor. Phys.* **51** (1974), 399.
- 13) R. Collins, *Phase Transitions and Critical Phenomena*, edited by Domb and Green (Academic Press, New York, 1972), Vol. 2, p. 271.
- 14) N. Ogita, A. Ueda, T. Ogawa, Y. Hiwatari and H. Matsuda, *Bussei Kenkyu* (mimeographed circular in Japanese) **24** (1975), A90.
- 15) M. J. Mandell, J. P. McTague and A. Rahman, *J. Chem. Phys.* **64** (1976), 3699.
- 16) M. Tanemura and T. Ogawa, *Bussei Kenkyu* **24** (1975), A98.
- 17) T. Ogawa and M. Tanemura, *Bussei Kenkyu* **22** (1974), H30.
- 18) E. C. Bain, *Trans. AIME* **70** (1924), 25.